Kwiryn Wojsyk, Agata Merda, Klaudia Klimaszewska, Paweł Urbańczyk, Grzegorz Golański

Microstructure and Mechanical Properties of Welded Joints in Austenitic Steel TP347HFG after Operation

Abstract: The analysis involved a similar welded joint made of steel TP347HFG after operation at a temperature of 580°C. Tests revealed that the primary mechanisms responsible for the degradation of the microstructure in all areas of the joint subjected to analysis were precipitation processes within the grains and along the grain boundaries. The grain boundaries contained two morphologies forming a continuous lattice. Precipitation processes resulted in the high tensile strength of the joint and high hardness within the weld face area. After operation, the test joint was characterised by relatively high impact energy, which could be attributed to the fine-grained microstructure and the presence of numerous annealing twins.

Keywords: welded joint, steel TP347HFG, microstructure, mechanical properties

DOI: *10.17729/ebis.2020.6/7*

Introduction

Materials used to make pressure elements of power unit systems are designed and manufactured so that they could transfer constant and cyclically variable thermomechanical loads during long-lasting operation. Requirements concerning the aforesaid materials are increasingly high because of the necessary transferring of high parameters of transported media and expected corrosion resistance triggered by exposure to flue gas or steam. Presently, elements of power units are made not only of low-alloy high-temperature creep resisting steels but also of advanced martensitic and austenitic steel grades. Newly developed high-temperature creep resisting steels implemented in power engineering systems are characterised by the presence of numerous alloying elements of various concentration. In cases of austenitic steels, the foregoing is tied to their operation at temperature exceeding 620 C. The appropriate chemical composition of such materials should ensure the high stability of the microstructure and the obtainment of mechanical properties enabling long-lasting operation. The thermodynamically unstable structure of austenitic steels during operation results in their gradually progressing degradation, adversely affecting both

dr inż. Kwiryn Wojsyk (PhD (DSc) Eng.) – Częstochowa University of Technology, Faculty of Mechanical Engineering and Computer Science; mgr inż. Agata Merda (MSc Eng.); mgr inż, Klaudia Klimaszewska (MSc Eng.); dr hab. inż. Grzegorz Golański (PhD (DSc) Habilitated Eng.), Professor at Częstochowa University of Technology, Faculty of Production Engineering and Materials Technology; dr inż. Paweł Urbańczyk(PhD (DSc) Eng.) – Office of Technical Inspection, Dąbrowa Górnicza

mechanical properties and corrosion resistance. For this reason, it is necessary to monitor, e.g. during scheduled repairs or diagnostic tests, the service life of such steels after many years of operation. The foregoing refers both to high-temperature creep resisting alloys and welded joints made of them [1–3]. The research work discussed in this article involved the analysis of the microstructure and tests of mechanical properties of a similar joint (after operation) made in austenitic steel TP347HFG.

Test materials and methodology

An element subjected to metallurgical tests was a welded joint in a steam superheater coil made of austenitic steel TP347HFG, for more than 54000 hours exposed to a temperature of 580°C and a pressure of 5.3 MPa. The scope of the tests included the following:

- analysis of the chemical composition of the base material performed using a SpectroLab spark emission spectrometer and the analysis of the chemical composition of the filler metal performed using an Jeol JSM6610LV scanning electron microscope (SEM) provided with an EDS attachment;
- cross-sectional macroscopic tests of the test welded joint performed using an Olympus SZ61 light microscope;
- microstructural tests performed using an Axiovert 25 light microscope and an SEM Jeol JSM6610LV scanning electron microscope; the test joint was subjected to etching in the Mi19Fe metallographic reagent;
- Vickers hardness test performed using an FV–700 hardness tester and an indenter load of 10 kG (98;1 N); hardness measurements were performed in two lines, i.e. on the weld face and weld root side;
- measurements of impact energy performed using a Charpy pendulum machine and standard specimens with a V-notch;
- static tensile tests performed using a Zwick Roel Z100 testing machine.

Table 1. Chemical composition of steel TP347HFG, %

C	Si	Mn	P	S	Cr	Ni	Nb	N	Mo
0.10	0.48	1.54	0.005	0.001	18.79	12.23	0.58	0.04	0.24

Table 2. Chemical composition of the filler metal, %

Element	Mn	Si	Cr	Ni	Nb	Fe
Face	1.28	0.56	19.32	10.16	0.67	68.02
Root	1.54	0.64	19.96	10.22	0.45	67.19

The chemical composition of the base material is presented in Table 1, whereas the chemical composition of the weld is presented in Table 2.

Macroscopic tests

The macroscopic image of the test welded joint is presented in Figure 1. The macroscopic observations revealed the proper structure of the joint. The joint did not contain any welding imperfections inconsistent with quality level B of standard [4].

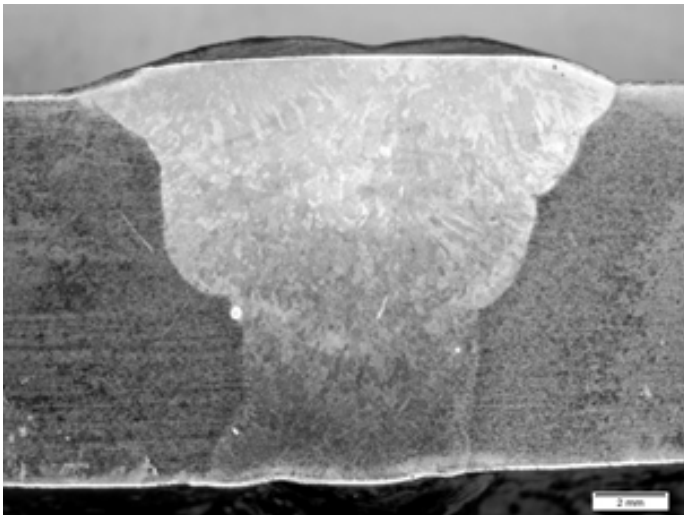

Fig. 1. Macroscopic image of the test welded joint

Microstructural tests

The microstructure of steel TP347HFG is presented in Figure 2. The test steel was characterised by the fine-grained austenitic microstructure with the grain size being 8/7 (according to ASTM scale) and annealing twins. As regards austenitic steels, the fine-grained structure is advantageous in terms of plasticity (ductility) and corrosion resistance. Tests discussed in publications [1, 5] revealed that

fine-grained austenitic steels are characterised by creep resistance comparable with that of coarse-grained steels. The microstructure of the test steel contained both twins coherent and those incoherent with the matrix. In austenitic steels, twins play an important role by dividing a homogenous austenite grain, and, as a result, refining the microstructure and reducing susceptibility to brittle cracking [6]. The microstructure of the test steel also contained numerous and large primary precipitates, locally arranged in bands. The EDS-based analysis revealed that the precipitates were rich primarily in niobium (Fig. 3). According to publication [7], the primary precipitates in steel TP347HFG are particles rich in niobium (NbC). The microstructure of austenitic steels stabilised using a highly carbide-forming element, e.g. niobium, is characterised by the presence of characteristic numerous and large primary precipitates. Because of their size, the role of such precipitates is, in practice, reduced to the bonding of carbon and/or nitrogen atoms as well as to inhibiting the growth of grains during the thermomechanical process. Such precipitates are characterised by high stability. According to publication [8], primary particles are disadvantageous precipitates as, during operation, the nucleation of microcracks may take place along their interphase boundary. In addition, the microstructure contains numerous precipitates of diverse morphology along grain boundaries, locally forming the so-called the continuous lattice of precipitates. Along twin boundaries it was also possible to observe single particles, whereas within grains it was possible to notice numerous precipitates. The primary degradation processes affecting high-temperature creep resisting austenitic steels taking place during operation include the precipitation processes of secondary phases [6, 9]. Privileged precipitation areas are grain boundaries, which primarily results from faster diffusion within these areas [8, 10].The grain boundaries of the test steel contained two morphologies of precipitates, i.e. numerous and relatively small precipitates and single large particles. Research performed by the authors of publication [7] and information contained in reference publications [11] imply that the above-named relatively small precipitates are $M_{23}C_6$ carbides. In the second case, the precipitates located at the tripoint of three grain boundaries were (because of their shape) probably the precipitates of phase σ. The precipitates of phase σ could be rich in chromium, iron and silicon (which was demonstrated by the EDS-based analysis (Fig. 4)). According to publication [12], silicon is a chemical element favouring the nucleation and the precipitation of phase σ in austenitic steels. An increase in a silicon content leads to an increase in the volume fraction of phase σ after operation [12]. The enrichment of phase σ in silicon was also observed in steel T321H after

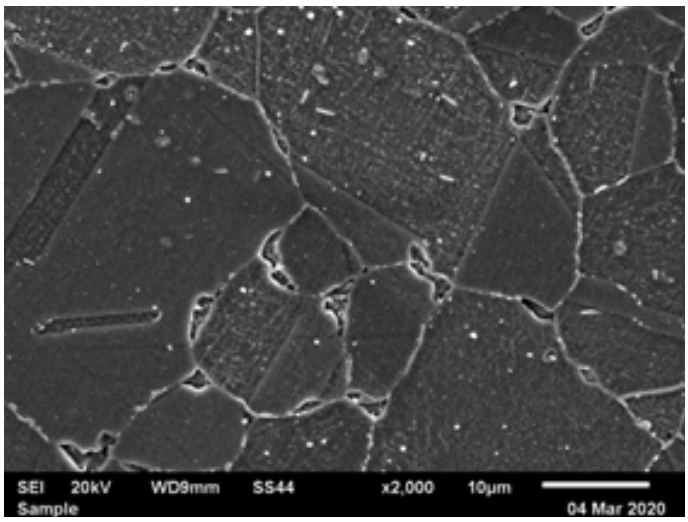

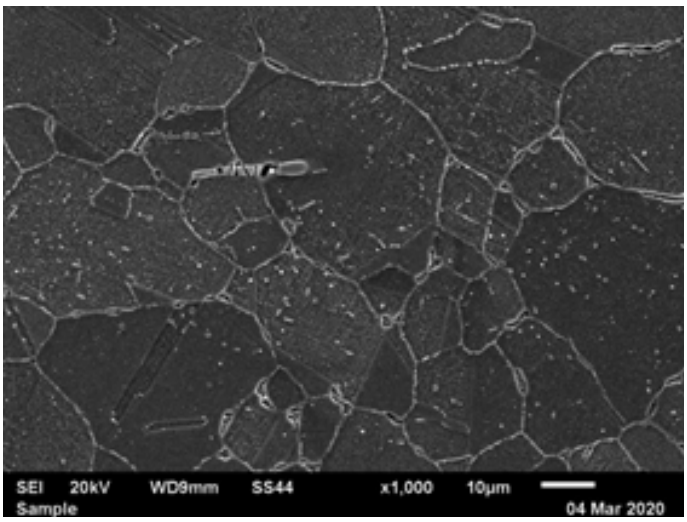

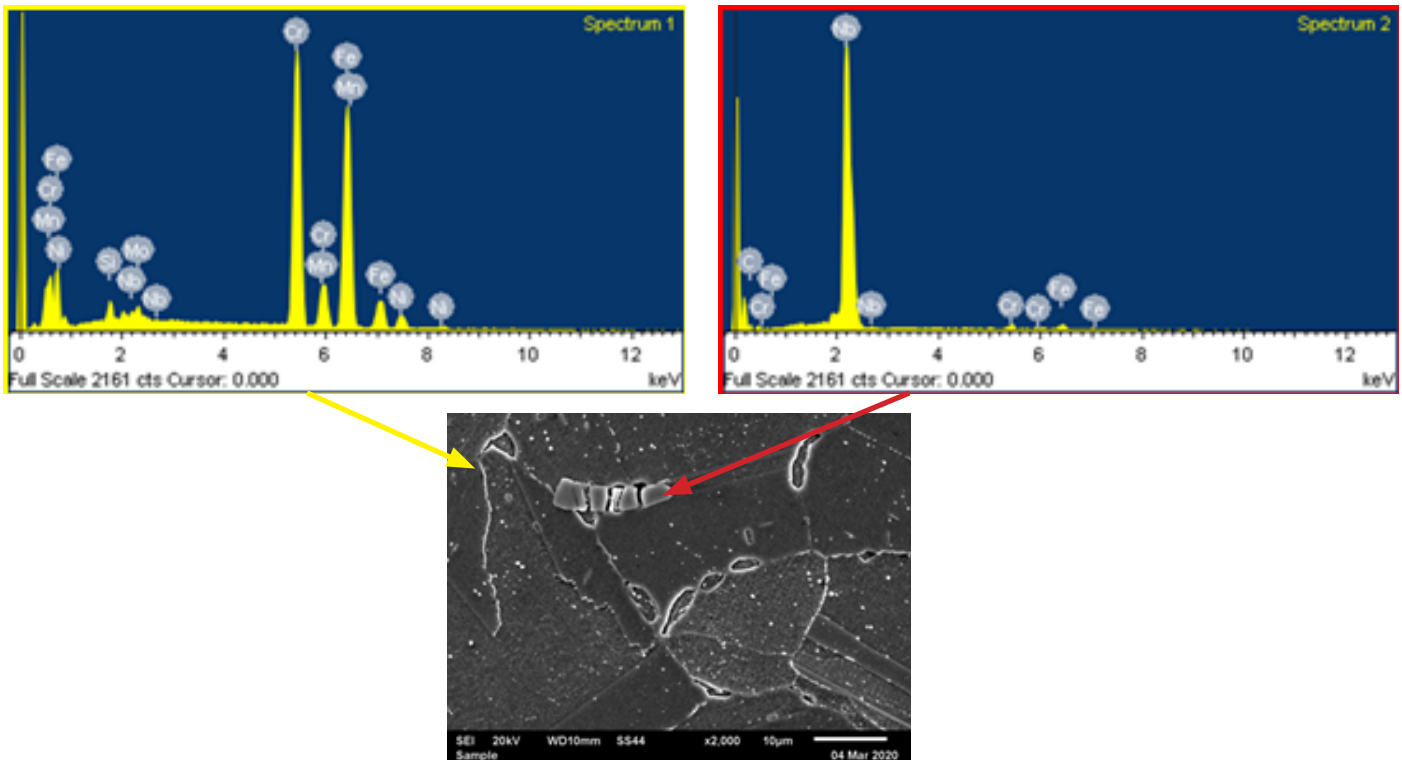

Fig. 3. Analysis (EDS) of precipitates

long-lasting operation [13]. The precipitation of M23C6 carbides in austenitic steels is connected with the ultimate solubility of carbon in the matrix [8, 10]. The above-named precipitates, in their dispersive form, [14] play a positive role by increasing creep resistance through the inhibition of glide along grain boundaries. However, the long-lasting operation of austenitic steels leads to an increase in the number and size of the precipitates along grain boundaries and the loss of the favourable effect of the former. Numerous particles rich in chromium and locally forming the continuous lattice of precipitates along grain boundaries may increase the sensitivity of austenitic steels to intercrystalline corrosion [15]. Intermetallic phase σ is an unfavourable precipitate in austenitic steels as its presence results not only in the reduction of plasticity or toughness but also in decreased corrosion resistance [16, 11]. Precipitates observed within grains were near-circular and acicular. Steel TP347HFG-related test results discussed in [7, 17] revealed the presence of numerous dispersive secondary NbC (NbX) precipitates within grains. Such precipitates effectively impede dislocations and significantly

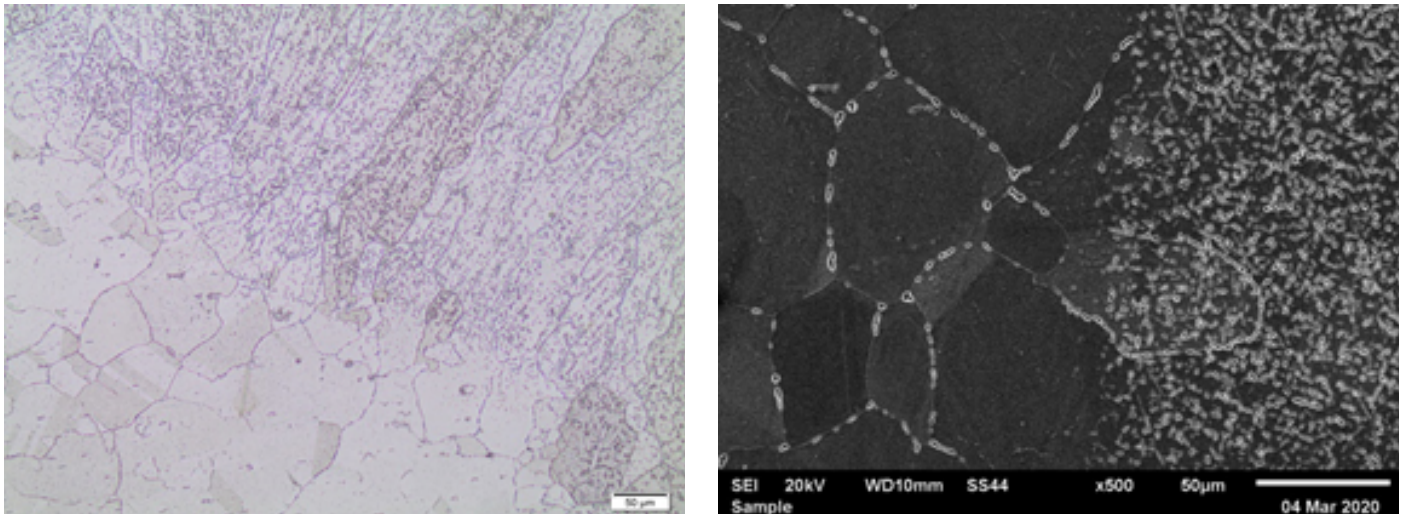

Fig. 4. Area near the fusion line of the test welded joint

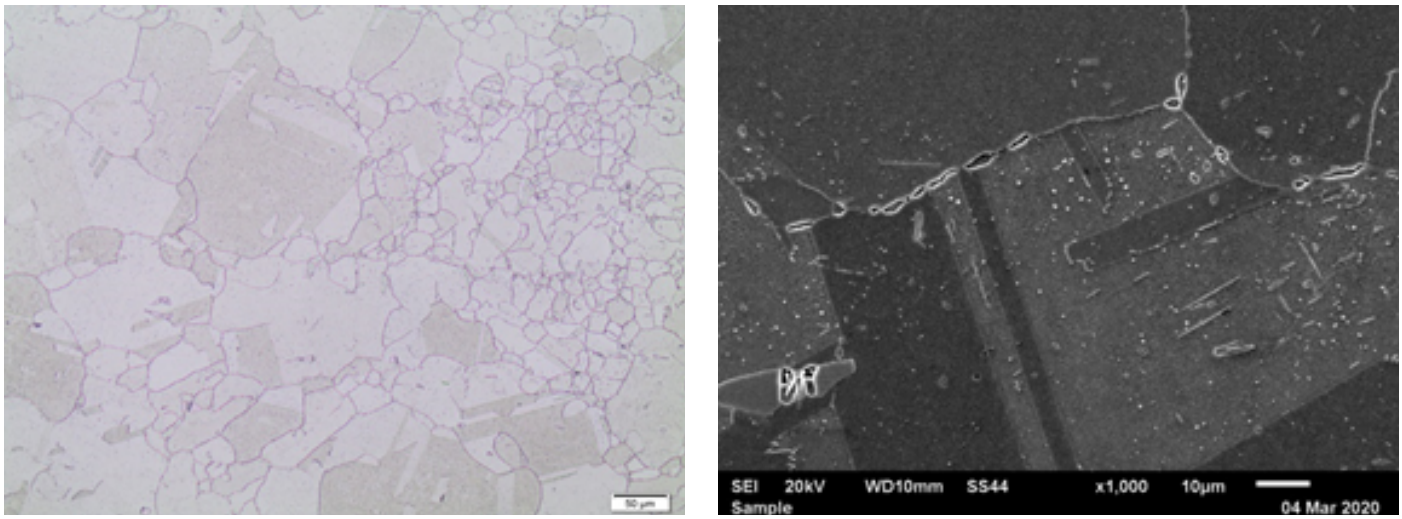

Fig. 5. Heat affected zone of the test welded joint

harden the material, not only increasing the yield point but also creep resistance. In turn, the morphology of the precipitates within grains implies that they were, most probably, M23C6, particles and phase σ. The presence of the precipitates within the grains was responsible for increased hardening and, consequently, affected mechanical properties and hardness. By contrast with the base material, the HAZ was characterised by grain growth, resulting from the welding process (Fig. 4). The grain size in the HAZ was 5/4. Similar to the base material, the microstructure of the HAZ contained numerous precipitates within the grains and along the grain boundaries. The size of the precipitates in the HAZ was similar to that of the precipitates observed in the base material. On the face side, the weld was characterised by the presence of numerous precipitates (of varied morphology) within the grains and the continuous lattice of precipitates along the grain boundaries/crystallites (Fig.5a). Similarly, on the root side it was also possible to observe precipitates within the crystallites and along their boundaries, yet their density was significantly lower (Fig. 5b). The difference in the density of the precipitates could probably be attributed to the diverse distribution of temperature across the joint thickness.

Tests of mechanical properties

The operation of high-temperature creep resisting steels not only triggers changes in their microstructure but also affects their mechanical

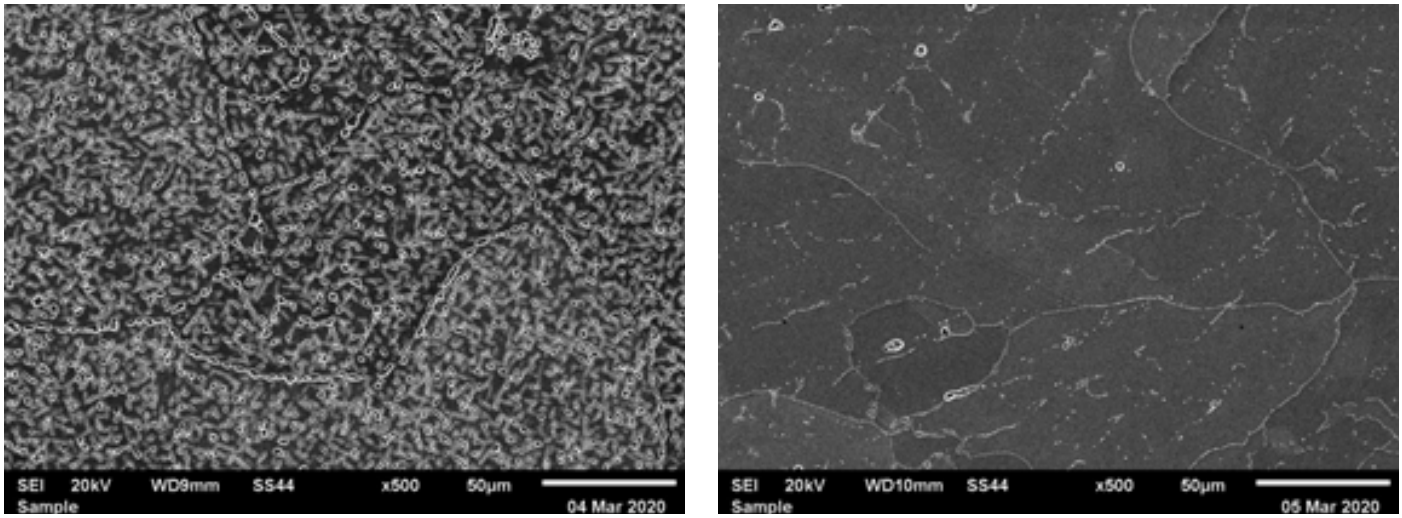

Fig. 6. Weld area of the test welded joint a) on the face side and b) on the root side

properties. Austenitic steels are supplied in the supersaturated state, responsible for good plastic properties and high toughness, yet relatively low mechanical properties [11]. Changes taking place in the microstructure during operation, such as the precipitation of secondary phases ($M_{23}C_6$, NbX, phase σ) lead to precipitation hardening, the increase of which depends on types of precipitates, their dispersion and arrangement. The presence of numerous precipitates in the microstructure translates into high mechanical properties. The tensile strength of the test joint at room temperature amounted to 814 MPa and was by 50% higher than the minimum strength of the base material (R_{mmin} – 550 MPa [18]). The maximum tensile strength of steel TP347HFG amounts to 750 MPa [18]. The foregoing confirms the significant impact of precipitation hardening on the mechanical properties (i.e. their increase) of the test joint. In each area of the V-notch, the impact energy of the joint was higher than the minimum value (Fig. 7), which, as regards the test steel, is KV_{min}>85 J [18]. However, it should be noted that, despite the presence of numerous precipitates (locally forming the continuous lattice) and phase σ along the grain boundaries, the test joint was characterised by relatively high impact energy, which could be ascribed to the fine-grained structure and/or the continued presence of relatively numerous twins as regards the base material and the high number of twins as regards the HAZ. In austenitic steels, the size of grains significantly affects impact energy in relation to advanced precipitation processes. In turn, the toughness of the weld results from the high number of precipitates and the unfavourable arrangement (locally) of the crystallisation grains. The cross-sectional hardness measurement revealed that, in each area of the joint, hardness was lower than the ultimate hardness of this type of material, i.e. HV_{max} – 350 HV (Fig. 8). The higher hardness of the weld face area in comparison with that of the weld root area resulted from the higher density of precipitates in the aforesaid area (Fig. 5a).

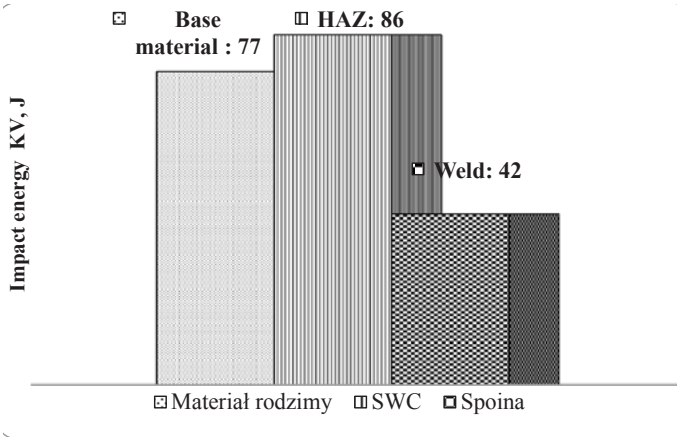

Fig. 7. Impact energy of the test joint

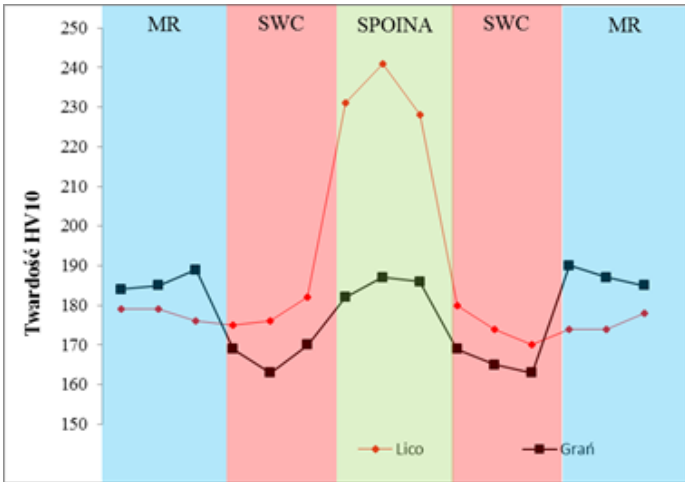

Fig. 8. Distribution of hardness in the cross section of the test welded joint

Conclusions

1. After long-lasting operation, the microstructure of the test welded joint contained numerous morphologically varied precipitates within the grains and along the grain boundaries.

2. The fine-grained microstructure and the presence of numerous annealing twins translated into the maintaining of the relatively high impact energy of the test joint in spite of the presence of the continuous lattice of precipitates along the grain boundaries.

References

[1] Barnard P.: Austenitic steel grades for boilers in ultra-supercritical power plants. Materials for ultra-supercritical and advanced ultra-supercritical power plants. [in] Di Gianfrancesco A.: Woodhead Publishing, 2017, pp. 99–119.

[2] Blicharski M.: Zmiany mikrostruktury w połączeniach spawanych różnoimiennych materiałów stosowanych w energetyce. Przegląd Spawalnictwa, 2013, no. 85, pp. 2–13.
[3] Brózda J.: Stale austenityczne nowej generacji stosowane na urządzenia energetyki o parametrach nadkrytycznych i ich spawanie. Biuletyn Instytutu Spawalnictwa, 2006, no. 50, pp. 40–48.
[4] PN-EN ISO 5817:2014-05 – Spawanie – Złącza spawane ze stali, niklu, tytanu i ich stopów (z wyjątkiem spawanych wiązką) – Poziomy jakości według niezgodności spawalniczych.
[5] Gibbons T. B.: Recent Advances in Steels for Coal Fired Power Plant: A Review. Transactions of the Indian Institute of Metals, 2013, no. 66, pp. 631–640.
[6] Zhang Z., Hu Z., Tu H.Y., Schmauder S.: Microstructure Evolution in HR3C Austenitic Steel during Long-term Creep at 6500C. Materials Science and Engineering A, 2016, no. 681, pp. 74–84.
[7] Golański G., Lis A. K., Słania J., Zieliński A.: Microstructural aspect of long term service of the austenitic TP347HFG steel. Archives of Metallurgy and Materials, 2015, no. 60, pp. 2901 – 2904.
[8] Sourmail T.: Precipitation in creep resistant austenitic stainless steels, Materials Science and Technology, 2001, no. 17, pp. 1–14.
[9] Wang B., Liu Z-h., Cheng S-h, Liu C-m., Wang J-z.: Microstructure evolution and mechanical properties of HR3C steel during long-term aging at high temperature. Journal of Iron and Steel Research International, 2013, no. 21, pp. 765–773.
[10] Padilha A. F., Rios P. R.: Decomposition of Austenite in Austenitic Stainless Steels. ISIJ International, 2002, no. 42, pp. 325–327.
[11] Zieliński A., Sroka M., Hernas A., Kremzer M.: The effect of long-term impact of elevated temperature on changes in microstructure and mechanical properties of HR3C steel. Archives of Metallurgy and Materials, 2016, no. 2, pp. 761–766.
[12] Lin D. Y., Chang T. Ch., Liu G. L.: Effect of Si contents on the growth behavior of σ phase in SUS 309L stainless steels. Scripta Materialia, 2003, no. 43, pp. 855–860.
[13] Purzyńska H., Golański G., Zieliński A., Dobrzański J., Sroka M.: Precipitation study in Ti-stabilised austenitic stainless steel after 207,000 h of service. Materials at High Temperatures, 2019, no. 36, pp. 296–303.
[14] Minami Y., Kimura H.: Effect of M23C6 and MC Carbides on the Creep Rupture Strength of 18% Cr-10%Ni-Ti-Nb Steel. Transactions ISIJ, 1987, no. 27, pp. 299–301.
[15] Yin Y., Faulkner R. G., Moreton P., Armson I., Coyle P.: Grain boundary chromium depletion in austenitic alloys. Journal of Materials Science, 2010, no. 45, pp. 5872–5882.
[16] Klementti K., Hanninen H., Kivilathi J.: The effect of sigma phase formation on the corrosion and mechanical properties of Nb- stabilized stainless steel cladding. Welding Research Supplement, 1984, no. 64, pp. 17–25.
[17] Erneman J., Schwind M., Andrén H. O., Nilsson J. O., Wilson A., Ågren J.: The evolution of primary and secondary niobium carbonitrides in AISI 347 stainless steel during manufacturing and long-term ageing. Acta Materialia, 2006, no. 54, pp. 67–76.
[18] Golański G., Zieliński A., Pietryka I., Urbańczyk P.: Stale do pracy w podwyższonej temperaturze. Wydawnictwo Politechniki Częstochowskiej, Częstochowa, 2018.